

Determination of sectorially best-fitting isotropic background media

C. Vanelle and D. Gajewski

email: vanelle@dkrz.de

keywords: anisotropy, perturbation method, background media

ABSTRACT

Computations in anisotropic media are commonly simplified by applying perturbation methods. These require suitable background media, that are often chosen to be isotropic. In this paper we present expressions for sectorially best-fitting isotropic P- and S-velocities. The equations follow from a generalisation of Fedorov's (1968) technique. Examples for media with polar (VTI) and triclinic symmetry confirm the superiority of the results over the commonly used globally best-fitting isotropic velocities by Fedorov (1968). This makes the method particularly suited for any application associated with perturbation techniques for anisotropic wave propagation.

INTRODUCTION

Computations in anisotropic media are usually very cumbersome. Many techniques developed for isotropic media will fail or have to be altered in the presence of anisotropy. Therefore, computations in anisotropic media are commonly simplified by applying perturbation methods (e.g., Jech and Pšenčík, 1989), where the anisotropic medium is described by a linear combination of a suitable background or reference medium, and a small perturbation with respect to the background medium. Often an isotropic background is assumed, where the perturbations account for the anisotropy. This has the advantage that isotropic techniques can be used for the computations in the background medium. In the simplest case, the isotropic velocities can be obtained from averaging the elastic constants over all phase directions, leading to the well-known result by Fedorov (1968). For applications like the generation of traveltimes with finite-difference methods in combination with perturbation (e.g., Ettrich and Gajewski, 1998; Soukina et al., 2003) Ettrich et al. (2001) have derived expressions for background media with elliptical anisotropy that permit to consider media with stronger anisotropy than isotropic backgrounds. However, their results are restricted to P-waves.

The results from Ettrich et al. (2001) were not only derived for averaging over all phase directions, but also for an average over a cone around the vertical axis, thus leading to a sectorially best-fitting elliptical background medium. Intuitively a sectorial fit permits a closer approximation when information on the phase directions can be restricted to a sector instead of the whole unit sphere. This is often possible, for example in the reflection/transmission problem, where Snell's law has to be evaluated at a boundary between two anisotropic media. In this case the horizontal slowness, and thus the azimuth angle is known, therefore averaging could be restricted to be carried out over the inclination only. Formulae for this type of averaging are provided in this work.

We have derived expressions for sectorially best-fitting isotropic velocities following the approach suggested by Fedorov (1968). These are closely related to the velocities resulting from the weak anisotropy approximation (Backus, 1965). In contrast to Ettrich et al.'s (2001) work we give also expressions for best-fitting shear velocities. Also, the averaging can take place over any region desired, not only over a cone around the vertical axis, although this important case is a subset of our solution.

In the first section of this paper, we describe Fedorov's (1968) averaging approach to obtain the globally best-fitting isotropic medium. We use a generalisation of his approach to determine a sectorially best-fitting medium. We demonstrate the superiority of the resulting expressions over the global average in the following section with examples on compressional and shear velocities and slowness surfaces for media with polar and triclinic symmetry. Finally, we summarise our conclusions and give an outlook.

METHOD

For the derivation of expressions for best-fitting isotropic background (or reference) velocities we follow the derivation for the globally best-fitting isotropic medium given in Fedorov (1968). We begin with the Christoffel matrix $\underline{\Lambda}$

$$\Lambda_{ik} = a_{ijkl} n_j n_l \quad , \quad (1)$$

where the a_{ijkl} are the elements of the density-normalised elasticity tensor, and the n_j are the components of the phase normal vector,

$$\mathbf{n} = \begin{pmatrix} \sin \theta \cos \phi \\ \sin \theta \sin \phi \\ \cos \theta \end{pmatrix} \quad , \quad (2)$$

where θ is the inclination and ϕ the azimuth angle. The eigenvalue problem for $\underline{\Lambda}$ leading to the three phase velocities V_m ($m=1,2,3$) is

$$(\Lambda_{ik} - V_m^2 \delta_{ik}) g_i^{(m)} = 0 \quad . \quad (3)$$

In (3), the eigenvector $g_i^{(m)}$ is the polarisation vector of the wave corresponding to the phase velocity V_m , which, in turn, is the m -th eigenvalue of $\underline{\Lambda}$. If the phase normal n_j is known, (3) can be solved and the phase velocities can be obtained in a closed form from $|\Lambda_{ik} - V_m^2 \delta_{ik}| = 0$ (e.g., with Cardani's formula).

Now we express the elasticity tensor a_{ijkl} in a linearised form by the sum of the elasticity tensor of an isotropic background medium, $a_{ijkl}^{(0)}$, and the deviations Δa_{ijkl} of the anisotropic medium from the isotropic background:

$$a_{ijkl} = a_{ijkl}^{(0)} + \Delta a_{ijkl} \quad . \quad (4)$$

Remembering that the elasticity tensor for an isotropic medium is given by

$$a_{ijkl}^{(0)} = (V_P^2 - 2V_S^2) \delta_{ij} \delta_{kl} + V_S^2 (\delta_{ik} \delta_{jl} + \delta_{il} \delta_{jk}) \quad (5)$$

we want to find the P- and S-wave velocities V_P and V_S that give the best isotropic approximation for an arbitrarily anisotropic medium.

To obtain this best-fitting isotropic background medium, it is required that

$$\langle (\Lambda_{ik} - \Lambda_{ik}^{(0)})^2 \rangle \stackrel{!}{=} \text{Min.} \quad (6)$$

becomes minimal (Fedorov, 1968). The brackets $\langle \rangle$ denote the averaging process

$$\langle A(\theta, \phi) \rangle_{\theta, \phi} = \frac{\int_{\phi_1}^{\phi_2} \int_{\theta_1}^{\theta_2} A(\theta, \phi) \sin \theta \, d\theta \, d\phi}{\int_{\phi_1}^{\phi_2} \int_{\theta_1}^{\theta_2} \sin \theta \, d\theta \, d\phi} \quad . \quad (7)$$

Expanding the square in (6) leads to

$$\langle (\Lambda_{ik} - \Lambda_{ik}^{(0)})^2 \rangle = \langle \Lambda_{ik} \Lambda_{ik} \rangle + \langle \Lambda_{ik}^{(0)} \Lambda_{ik}^{(0)} \rangle - 2 \langle \Lambda_{ik} \Lambda_{ik}^{(0)} \rangle \quad , \quad (8)$$

where

$$\Lambda_{ik}^{(0)} \Lambda_{ik}^{(0)} = V_P^4 + 2V_S^4 \quad , \quad (9)$$

and

$$\Lambda_{ik}\Lambda_{ik}^{(0)} = (V_P^2 - V_S^2)a_{ijkl}n_in_jn_kn_l + V_S^2a_{ijil}n_jn_l \quad . \quad (10)$$

To minimise the objective function (6), the derivatives of (6) with respect to V_P and V_S must be zero. The resulting linear system of equations leads to

$$\begin{aligned} V_P^2 &= a_{ijkl}\langle n_in_jn_kn_l \rangle \quad , \\ V_S^2 &= \frac{1}{2} (a_{ijkl}\langle n_jn_l \rangle - V_P^2) \quad . \end{aligned} \quad (11)$$

These isotropic phase velocities yield the best-fitting background velocities in a least-square sense.

The same result was originally derived by Fedorov (1968) following the same approach, but minimising (6) not for the velocities but for the Lamé-parameters λ and μ instead. Fedorov derived his results in order to find *that isotropic medium that is most similar to the given crystal not only as regards the propagation of elastic waves but also as regards elastic properties generally*. To do so, he averaged the phase normals n_j over the entire unit sphere, i.e. $\theta = [0 \dots \pi]$ and $\phi = [0 \dots 2\pi]$, in (7), resulting in

$$\begin{aligned} V_P^2 &= \frac{1}{15} (a_{iikk} + 2 a_{ikik}) \quad , \\ V_S^2 &= \frac{1}{30} (3 a_{ikik} - a_{iikk}) \quad . \end{aligned} \quad (12)$$

Fedorov (1968) has also determined the best-fitting isotropic velocities for the case that the direction of the phase normal was fixed, i.e. no averaging was carried out in Equation (11). In this case the resulting velocities coincide with those obtained from the weak anisotropy approximation (Backus, 1965). More precisely, for the S-wave the best-fitting isotropic velocity is the geometric mean of the weak anisotropy qS_1 - and qS_2 -velocities:

$$\begin{aligned} V_{PWA}^2 &= a_{ijkl} n_in_jn_kn_l \\ V_{SWA}^2 &= \frac{1}{2} (a_{ijik} n_jn_k - V_{PWA}^2) \quad . \end{aligned} \quad (13)$$

This result is not surprising as the weak anisotropy approximation is based on a linear (first-order) perturbation of the elasticity tensor, as is Equation (4).

There are, however, situations where neither the average over the whole unit sphere nor the result for a given phase direction is the best choice for a background medium. This is, for example, the case when only two of the three components of p_j are available, as for the reflection-transmission problem at an interface, where a sixth-order polynomial must be solved to evaluate Snell's law (Henneke, 1971). Another example is the second-order interpolation of traveltimes (Vanelle and Gajewski, 2002) in the presence of topography. Here, the vertical slowness is required for the interpolation, but only the horizontal components are available. The same problem occurs in the determination of geometrical spreading from traveltimes (Vanelle and Gajewski, 2003). In all these cases, only the horizontal slowness is known. Since the phase velocity is also unknown, the vertical slowness can not simply be obtained from the eikonal equation. Here, it would be a better choice to use a background medium that is obtained only from averaging over the inclination angle θ since the azimuth angle ϕ is known.

Also, for other applications using perturbation methods, it can be favourable to use a sectorially best-fitting background medium rather than the global one given by (12). This has been recognised before, for example by Ettrich et al. (2002) who have published equations for approximate P-wave velocities that yield the best fit for a cone around the vertical axis.

Therefore we have generalised Fedorov's (1968) result for the cases in between averaging over the whole unit sphere and no averaging at all. As the resulting expressions are longish we have decided to accumulate them in appendices rather than in the main text. Appendix A gives the results for an average

over a sectorial fit in θ and ϕ (Equations (16) and (17)). In Appendix B results are given where the average is only taken over the inclination for those applications where the azimuth is known (Equations (18) and (19)). Finally, Appendix C gives the results for the special case of a weakly anisotropic medium with polar symmetry (VTI medium) in terms of Thomsen's (1986) parameters. The abbreviations used in Appendices A to C are summarised in Appendix D.

In the next section we will give examples for the quality of the fit that can be obtained by using a sectorial approximation.

EXAMPLES FOR SECTORIALLY BEST-FITTING ISOTROPIC BACKGROUND MEDIA

We consider two different types of anisotropic media to demonstrate the sectorially best-fitting isotropic background velocities. The first is a medium with polar symmetry and the vertical axis as symmetry axis (this symmetry is also known as vertically transverse isotropic, VTI). The density-normalised elastic parameters for this synthetic medium matching a shale (see, e.g., Thomsen, 1986) are

$$\underline{\mathbf{A}} = \begin{pmatrix} 13.59 & 6.795 & 5.44 & 0. & 0. & 0. \\ & 13.59 & 5.44 & 0. & 0. & 0. \\ & & 10.873 & 0. & 0. & 0. \\ & & & 2.72 & 0. & 0. \\ & & & & 2.72 & 0. \\ & & & & & 3.4 \end{pmatrix}, \quad (14)$$

(values in km^2/s^2) or, in Thomsen's (1986) parameters:

$$\begin{aligned} \alpha &= 3.2974 \text{ km/s}, & \beta &= 1.6492 \text{ km/s}, \\ \epsilon &= 0.1249, & \gamma &= 0.1250, \\ \delta &= 0.0006. \end{aligned}$$

We have computed the globally best-fitting isotropic velocities and the isotropic velocities for fixed inclination and azimuth angles from Equations (12) and (13). As mentioned above, the latter correspond to the weak-anisotropy approximation. Finally, we have applied Equations (18) and (19) to obtain the sectorially best-fitting velocities for sectors of 30° width in inclination. (Due to the rotational symmetry around the vertical axis the results from (18) and (19), and (16) and (17) coincide.) All results are displayed together with the exact solution in Figure 1 for the P-wave and Figure 2 for the shear wave.

It can be immediately seen that for the P-wave the 30° width sectorial fit is far superior to the global approximation (Figure 1, left). This is also confirmed by the slowness surface plot in the right of Figure 1. Here, only the result for the averaging from 0° to 30° is shown together with the exact values and the global approximation. It is obvious from Figure 1 that in the 30° cone around the vertical axis the sectorial fit yields a much better approximation than the global one. For P-waves this was also shown by Ettrich et al. (2001).

At a first glance, the results appear less convincing for the shear wave in Figure 2, however, we should not expect that we can approximate two different anisotropic shear velocities with one isotropic velocity that fits both well. Also, the velocity range displayed in the shear velocity plot is smaller than that in the P-velocity plot, therefore the deviations appear even larger. If we take a closer look, we still find that the sectorial fit matches the exact velocities better than the global one. This can also be seen in the plot of the slowness surface in the right of Figure 2.

We have computed phase velocities and slowness surfaces in the same manner for a second example, a sandstone with triclinic symmetry (Mensch and Rasolofosaon, 1997). It is described by the density-

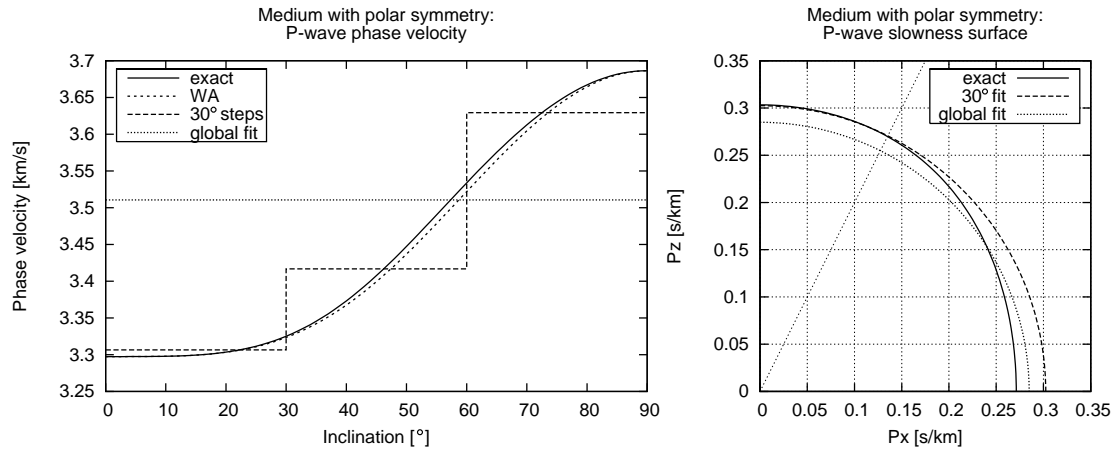


Figure 1: P-wave phase velocities (left) and slowness surfaces (right) for a medium with polar symmetry. In the phase velocity plot, WA is short for the weak anisotropy approximation. In the slowness surface plot, the 30° line corresponds to an average over θ in the range $[0^\circ \dots 30^\circ]$. The thin dotted line indicates the 30° cone.

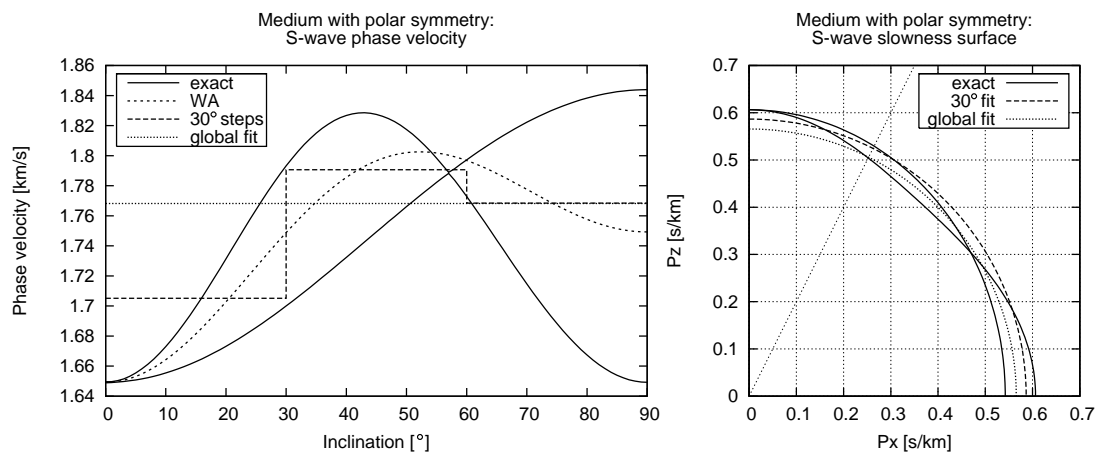


Figure 2: Shear wave phase velocities (left) and slowness surfaces (right) for a medium with polar symmetry. In the phase velocity plot, WA is short for the weak anisotropy approximation. In the slowness surface plot, the 30° line corresponds to an average over θ in the range $[0^\circ \dots 30^\circ]$. The thin dotted line indicates the 30° cone.

normalised elastic parameters

$$\underline{\mathbf{A}} = \begin{pmatrix} 4.95 & 0.43 & 0.62 & 0.67 & 0.52 & 0.38 \\ & 5.09 & 1.00 & 0.09 & -0.09 & -0.28 \\ & & 6.77 & 0.00 & -0.24 & -0.48 \\ & & & 2.45 & 0.00 & 0.09 \\ & & & & 2.88 & 0.00 \\ & & & & & 2.35 \end{pmatrix} \quad (15)$$

(values are given in km^2/s^2). We have only considered the x_1 -direction with the azimuth angle $\phi = 0$ here. Figure 3 shows the resulting P-wave phase velocities (left) and slowness surfaces (right), Figure 4 shows the same for the shear waves.

As for the polar medium, we can see in Figure 3 (left) that again the sectorial fit for the P-wave is a much better approximation to the real phase velocity than the global fit. In the slowness surface plot (right), we have displayed two sectorial fits. First, we have averaged θ from $[-30^\circ \dots 30^\circ]$ and ϕ from $[-15^\circ \dots 15^\circ]$. The second fit (denoted as 30° fit) results from averaging in θ over the interval $[-30^\circ \dots 30^\circ]$ while keeping ϕ constant, i.e. $\phi = 0^\circ$. Although in this case both sectorial fits are very close to each other, larger differences can and do occur, for example if an azimuth angle of 60° is considered (not shown here). Both are superior to the approximation that results from averaging over all azimuths within the 30° cone around the vertical axis. For the shear wave we find again confirmed in Figure 4 that a single velocity value cannot correctly describe both anisotropic shear velocities although the sectorial fit is still a better approximation than the global one.

CONCLUSIONS AND OUTLOOK

We have presented expressions for sectorially best-fitting isotropic background media. These were obtained from a generalisation of Fedorov's (1968) method. Examples confirm that the sectorial approximation is generally superior to the global one. This conclusion is of special interest for applications within seismic exploration as here we are mainly concerned about a region restricted to inclinations below about 30° . Particularly for the P-waves we find good agreement between the real and the best-fitting isotropic background velocity resulting from the sectorial fit. But despite the fact that we cannot outwit physics by replacing two different shear velocities in the anisotropic medium by one isotropic background shear velocity, the results for the shear wave velocities are still very useful with regards to applications based on perturbation methods.

Possible applications are the second-order travelttime interpolation (Vanelle and Gajewski, 2002) in anisotropic media when topography occurs and the determination of geometrical spreading from traveltimes (Vanelle and Gajewski, 2003). Here, the sectorially best-fitting background media can be combined with perturbation method in an iterative procedure to determine the third, missing, slowness component. The initial results are very promising and will be published in a follow-up paper. They are of particular interest as the method can also be applied to shear waves. In a similar way, we can solve the reflection/transmission problem at an interface between two anisotropic media. Generally, the expressions for sectorially best-fitting isotropic background media are of interest for any application associated with perturbation methods for anisotropic wave propagation.

ACKNOWLEDGEMENTS

We thank the members of the Applied Geophysics Group in Hamburg for continuous discussions. This work was partially supported by the German Research Foundation (DFG, grants Va207/2-1 and Ga850/11-1) and the sponsors of the Wave Inversion Technology (WIT) Consortium.

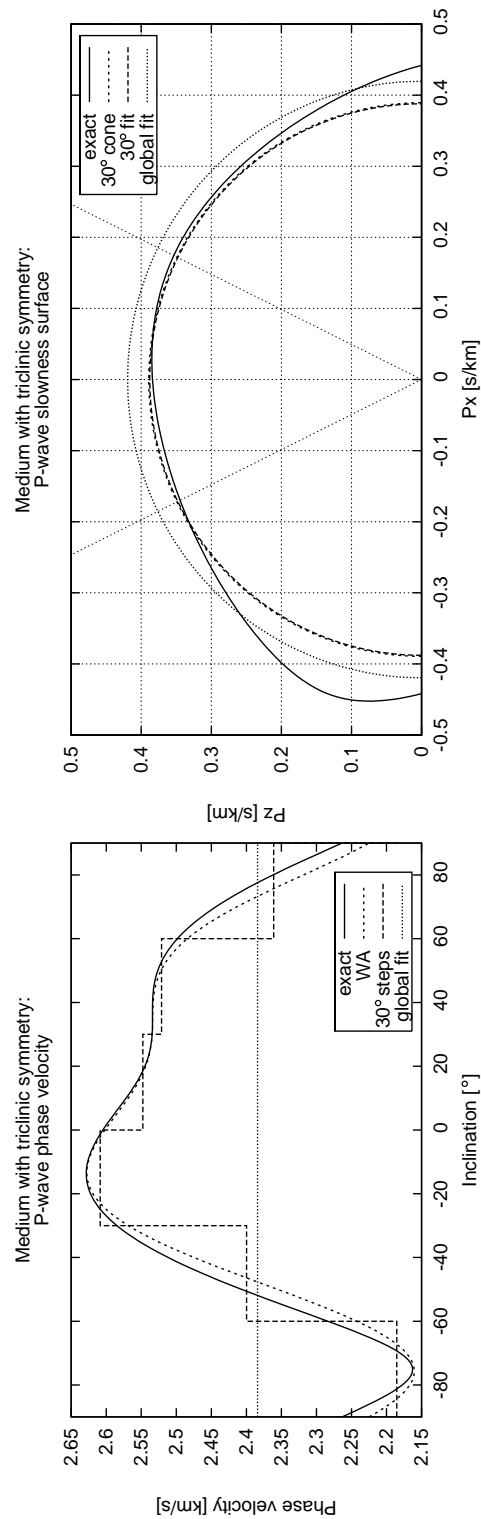


Figure 3: P-wave phase velocities (left) and slowness surfaces (right) for a medium with triclinic symmetry. In the phase velocity plot, WA is short for the weak anisotropy approximation. In the slowness surface plot, the 30° line corresponds to an average over θ in the range $[0^\circ \dots 30^\circ]$. The thin dotted line indicates the 30° cone.

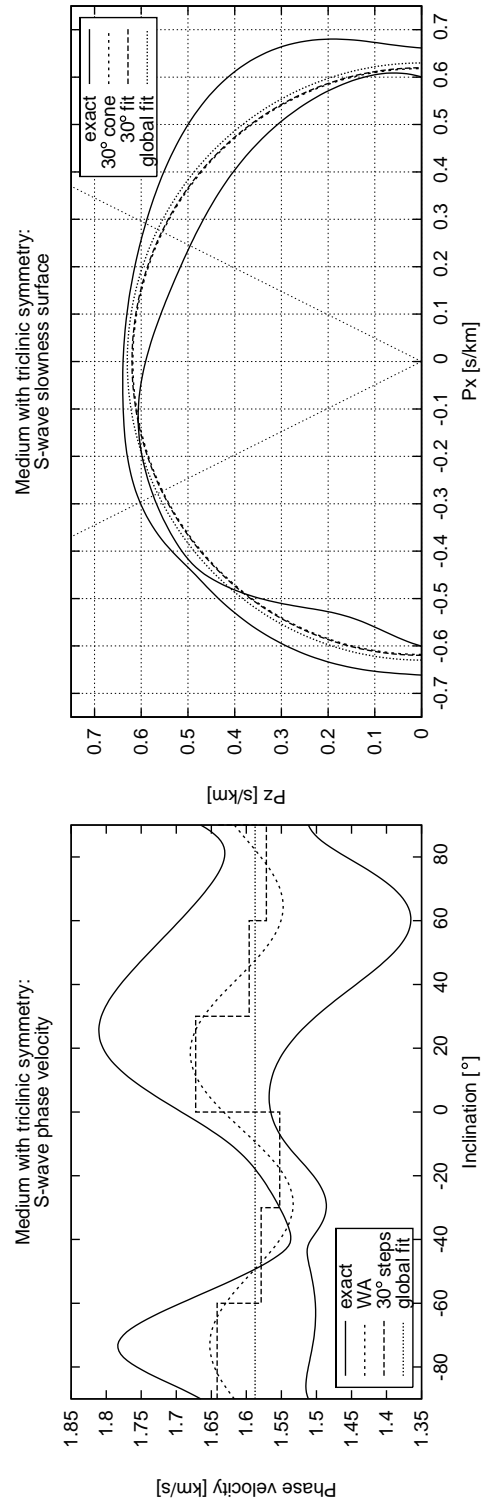


Figure 4: Shear wave phase velocities (left) and slowness surfaces (right) for a medium with triclinic symmetry. In the phase velocity plot, WA is short for the weak anisotropy approximation. In the slowness surface plot, the 30° line corresponds to an average over θ in the range $[0^\circ \dots 30^\circ]$. The thin dotted line indicates the 30° cone.

REFERENCES

- Backus, G. E. (1965). Possible forms of seismic anisotropy of the uppermost mantle under oceans. *Journal of Geophysical Research*, 70:3429–3439.
- Ettrich, N. and Gajewski, D. (1998). Traveltime computation by perturbation with fd-eikonal solvers in isotropic and weakly anisotropic media. *Geophysics*, 63:1066–1078.
- Ettrich, N., Gajewski, D., and Kashtan, B. M. (2001). Reference ellipsoids for anisotropic media. *Geophysical Prospecting*, 49:321–334.
- Fedorov, F. I. (1968). *Theory of Elastic Waves in Crystals*. Plenum Press, New York.
- Henneke, E. G. (1971). Reflection-refraction of a stress wave at a plane boundary between anisotropic media. *The Journal of the Acoustical Society of America*, 51:210–217.
- Jech, J. and Pšenčík, I. (1989). First-order perturbation method for anisotropic media. *Geophysical Journal International*, 99:369–376.
- Mensch, T. and Rasolofosaon, P. N. J. (1997). Elastic wave velocities in anisotropic media of arbitrary anisotropy – generalisation of thomsen’s parameters ϵ , δ , and γ . *Geophysical Journal International*, 128:43–63.
- Pšenčík, I. (1998). Green’s functions for inhomogeneous weakly anisotropic media. *Geophysical Journal International*, 135:279–288.
- Soukina, S. M., Gajewski, D., and Kashtan, B. M. (2003). Traveltime computation for 3d anisotropic media by a finite difference perturbation method. *Geophysical Prospecting*, 51:431–441.
- Thomsen, L. (1986). Weak elastic anisotropy. *Geophysics*, 51:1954–1966.
- Thomsen, L. (1993). Weak anisotropic reflections. In Castagna, J. and Backus, M., editors, *Offset dependent reflectivity*, pages 103–114. Society of Exploration Geophysicists, Tulsa.
- Vanelle, C. and Gajewski, D. (2002). Second-order interpolation of traveltimes. *Geophysical Prospecting*, 50:73–83.
- Vanelle, C. and Gajewski, D. (2003). Determination of geometrical spreading from traveltimes. *Journal of Applied Geophysics*, 54:in press.

APPENDIX A

In this appendix we provide the expressions for best-fitting isotropic background velocities, if the averaging is carried out over the inclination (θ) and the azimuth (ϕ) in the intervals $[\theta_1 \dots \theta_2]$ and $[\phi_1 \dots \phi_2]$. If

$-\theta_1 \neq \theta_2$, we find for the best-fitting P-velocity

$$\begin{aligned}
V_P^2 &= V_P^2(\theta_1, \theta_2, \phi_1, \phi_2) = a_{ijkl} \langle n_i n_j n_k n_l \rangle_{\theta, \phi} \\
&= A_{11} \left(\frac{C_1 - 2C_3 + C_5}{C_1} \right) \left(\frac{3\Delta_0 + \Delta_2 + \Delta_4}{8\Delta_0} \right) + A_{22} \left(\frac{C_1 - 2C_3 + C_5}{C_1} \right) \left(\frac{3\Delta_0 - \Delta_2 + \Delta_4}{8\Delta_0} \right) \\
&+ A_{33} \frac{C_5}{C_1} \\
&+ (4A_{44} + 2A_{23}) \left(\frac{C_3 - C_5}{C_1} \right) \left(\frac{4\Delta_0 - \Delta_2}{8\Delta_0} \right) + (4A_{55} + 2A_{13}) \left(\frac{C_3 - C_5}{C_1} \right) \left(\frac{4\Delta_0 + \Delta_2}{8\Delta_0} \right) \\
&+ (4A_{66} + 2A_{12}) \left(\frac{C_1 - 2C_3 + C_5}{C_1} \right) \left(\frac{\Delta_0 - \Delta_4}{8\Delta_0} \right) \\
&- 4A_{16} \left(\frac{C_1 - 2C_3 + C_5}{C_1} \right) \left(\frac{\Gamma_4}{8\Delta_0} \right) + 4A_{26} \left(\frac{C_1 - 2C_3 + C_5}{C_1} \right) \left(\frac{\Sigma_4}{8\Delta_0} \right) \\
&+ 4A_{24} \left(\frac{S_5}{C_1} \right) \left(\frac{\Gamma_1 - \Gamma_3}{8\Delta_0} \right) - 4A_{15} \left(\frac{S_5}{C_1} \right) \left(\frac{\Sigma_1 - \Sigma_3}{8\Delta_0} \right) \\
&+ 4A_{34} \left(\frac{S_3 - S_5}{C_1} \right) \left(\frac{\Gamma_1}{8\Delta_0} \right) - 4A_{35} \left(\frac{S_3 - S_5}{C_1} \right) \left(\frac{\Sigma_1}{8\Delta_0} \right) \\
&+ (4A_{14} + 8A_{56}) \left(\frac{S_5}{C_1} \right) \left(\frac{\Gamma_3}{8\Delta_0} \right) - (4A_{25} + 8A_{46}) \left(\frac{S_5}{C_1} \right) \left(\frac{\Sigma_3}{8\Delta_0} \right) \\
&- (4A_{36} + 8A_{45}) \left(\frac{C_3 - C_5}{C_1} \right) \left(\frac{\Gamma_2}{8\Delta_0} \right), \tag{16}
\end{aligned}$$

and for the best-fitting shear velocity

$$\begin{aligned}
V_S^2 &= V_S^2(\theta_1, \theta_2, \phi_1, \phi_2) = \frac{1}{2} (a_{ijkl} \langle n_j n_l \rangle_{\theta, \phi} - V_P^2) \\
&= A_{11} \left(\frac{C_1 - C_3}{2C_1} \right) \left(\frac{4\Delta_0 + \Delta_2}{8\Delta_0} \right) + A_{22} \left(\frac{C_1 - C_3}{2C_1} \right) \left(\frac{4\Delta_0 - \Delta_2}{8\Delta_0} \right) + A_{33} \left(\frac{C_3}{2C_1} \right) \\
&+ A_{44} \left[\left(\frac{C_1 - C_3}{2C_1} \right) \left(\frac{4\Delta_0 - \Delta_2}{8\Delta_0} \right) + \frac{C_3}{2C_1} \right] + A_{55} \left[\left(\frac{C_1 - C_3}{2C_1} \right) \left(\frac{4\Delta_0 + \Delta_2}{8\Delta_0} \right) + \frac{C_3}{2C_1} \right] \\
&+ A_{66} \left(\frac{C_1 - C_3}{2C_1} \right) + 2(A_{16} + A_{26} + A_{45}) \left(\frac{C_1 - C_3}{2C_1} \right) \left(\frac{\Sigma_2}{8\Delta_0} \right) \\
&+ 2(A_{24} + A_{34} + A_{56}) \left(\frac{S_3}{2C_1} \right) \left(\frac{\Gamma_1}{8\Delta_0} \right) - 2(A_{15} + A_{35} + A_{46}) \left(\frac{S_3}{2C_1} \right) \left(\frac{\Sigma_1}{8\Delta_0} \right) \\
&- \frac{V_P^2}{2}. \tag{17}
\end{aligned}$$

The abbreviations C_n , S_n , Γ_n , Σ_n , and Δ_n are introduced in Appendix D. In the special case that $\theta_1 = 0$, $\theta_2 = \pi$, $\phi_1 = 0$, and $\phi_2 = 2\pi$, these expressions reduce to the global average of Fedorov (1968) given by (12). For $\theta_1 = 0$, $\theta_2 = \theta$, $\phi_1 = 0$, and $\phi_2 = 2\pi$, Equation (16) is equal to the sectorially best-fitting isotropic P-velocity derived by Etrich et al. (2001).

If $-\theta_1 = \theta_2 = \theta$, Equations (16) and (17) must be used in a variant as C_1 becomes zero: In (16) and (17) we must replace C_n by C_n^0 and S_n by zero. The abbreviations C_n^0 can also be found in Appendix D.

APPENDIX B

If the phase normals are averaged over the inclination (θ) only, we only integrate over θ in (7). As result we find for the best-fitting P-velocity in the case that $-\theta_1 \neq \theta_2$

$$\begin{aligned}
V_P^2 &= V_P^2(\theta_1, \theta_2) = a_{ijkl} \langle n_i n_j n_k n_l \rangle_\theta \\
&= A_{11} \left(\frac{C_1 - 2C_3 + C_5}{C_1} \right) \cos^4 \phi + A_{22} \left(\frac{C_1 - 2C_3 + C_5}{C_1} \right) \sin^4 \phi + A_{33} \frac{C_5}{C_1} \\
&+ (4A_{44} + 2A_{23}) \left(\frac{C_3 - C_5}{C_1} \right) \sin^2 \phi + (4A_{55} + 2A_{13}) \left(\frac{C_3 - C_5}{C_1} \right) \cos^2 \phi \\
&+ (4A_{66} + 2A_{12}) \left(\frac{C_1 - 2C_3 + C_5}{C_1} \right) \sin^2 \phi \cos^2 \phi \\
&+ 4A_{16} \left(\frac{C_1 - 2C_3 + C_5}{C_1} \right) \sin \phi \cos^3 \phi + 4A_{26} \left(\frac{C_1 - 2C_3 + C_5}{C_1} \right) \cos \phi \sin^3 \phi \\
&- 4A_{24} \left(\frac{S_5}{C_1} \right) \sin^3 \phi - 4A_{15} \left(\frac{S_5}{C_1} \right) \cos^3 \phi \\
&- 4A_{34} \left(\frac{S_3 - S_5}{C_1} \right) \sin \phi - 4A_{35} \left(\frac{S_3 - S_5}{C_1} \right) \cos \phi \\
&- (4A_{14} + 8A_{56}) \left(\frac{S_5}{C_1} \right) \sin \phi \cos^2 \phi - (4A_{25} + 8A_{46}) \left(\frac{S_5}{C_1} \right) \cos \phi \sin^2 \phi \\
&+ (4A_{36} + 8A_{45}) \left(\frac{C_3 - C_5}{C_1} \right) \sin \phi \cos \phi, \tag{18}
\end{aligned}$$

and for the best-fitting shear velocity

$$\begin{aligned}
V_S^2 &= V_S^2(\theta_1, \theta_2) = \frac{1}{2} (a_{ijkl} \langle n_j n_l \rangle_\theta - V_P^2) \\
&= A_{11} \left(\frac{C_1 - C_3}{2C_1} \right) \cos^2 \phi + A_{22} \left(\frac{C_1 - C_3}{2C_1} \right) \sin^2 \phi + A_{33} \left(\frac{C_3}{2C_1} \right) \\
&+ A_{44} \left[\left(\frac{C_1 - C_3}{2C_1} \right) \sin^2 \phi + \frac{C_3}{2C_1} \right] + A_{55} \left[\left(\frac{C_1 - C_3}{2C_1} \right) \cos^2 \phi + \frac{C_3}{2C_1} \right] + A_{66} \left(\frac{C_1 - C_3}{2C_1} \right) \\
&+ 2(A_{16} + A_{26} + A_{45}) \left(\frac{C_1 - C_3}{2C_1} \right) \sin \phi \cos \phi \\
&- 2(A_{24} + A_{34} + A_{56}) \left(\frac{S_3}{2C_1} \right) \sin \phi + 2(A_{15} + A_{35} + A_{46}) \left(\frac{S_3}{2C_1} \right) \cos \phi \\
&- \frac{V_P^2}{2}. \tag{19}
\end{aligned}$$

The abbreviations C_n and S_n are introduced in Appendix D.

If $-\theta_1 = \theta_2 = \theta$, Equations (18) and (19) must be used in a variant as C_1 becomes zero: In (18) and (19) we must replace C_n by C_n^0 and S_n by zero. The abbreviations C_n^0 can also be found in Appendix D.

APPENDIX C

In this appendix we rewrite the expressions for the sectorially best-fitting velocities for the special case of an anisotropic medium with polar symmetry in terms of Thomsen's (1986) parameters. An anisotropic

medium with polar symmetry, also commonly addressed as vertical transverse isotropic (VTI) symmetry, is characterised by the elastic tensor

$$\underline{\mathbf{A}} = \begin{pmatrix} A_{11} & A_{11} - 2A_{66} & A_{13} & 0 & 0 & 0 \\ & A_{11} & A_{13} & 0 & 0 & 0 \\ & & A_{33} & 0 & 0 & 0 \\ & & & A_{55} & 0 & 0 \\ & & & & A_{55} & 0 \\ & & & & & A_{66} \end{pmatrix}.$$

We use Thomsen's parameters (Thomsen, 1986) and the weak anisotropy approximation for δ (Thomsen, 1993) to express the elastic parameters as

$$\begin{aligned} A_{11} &= \alpha^2(1 + 2\epsilon), & A_{33} &= \alpha^2, \\ A_{55} &= \beta^2, & A_{66} &= \beta^2(1 + 2\gamma), \\ A_{13} &= \alpha^2(1 + \delta) - 2\beta^2. \end{aligned}$$

Since the velocity is independent of the azimuth in this type of medium, Equations (16) and (17) lead to the same result as Equations (18) and (19), namely for the best-fitting P-wave velocity we get

$$V_P^2 = \alpha^2 \left[1 + 2 \frac{C_1 - 2C_3 + C_5}{C_1} \epsilon + 2 \frac{C_3 - C_5}{C_1} \delta \right], \quad (20)$$

and for the best-fitting S-wave velocity

$$V_S^2 = \beta^2 \left[1 + \frac{C_1 - C_3}{C_1} \gamma \right] + \alpha^2 \frac{C_3 - C_5}{C_1} (\epsilon - \delta). \quad (21)$$

The abbreviations C_1 , C_3 , and C_5 are introduced in Appendix D.

APPENDIX D

In this appendix we introduce the abbreviations used in the results. The averaging process described by Equation (7) leads to a set of integrals of trigonometric functions. In order to make the expressions for the velocities more legible we introduce the abbreviations

$$\begin{aligned} C_5 &= \frac{\cos^5 \theta_2 - \cos^5 \theta_1}{5}, & S_5 &= \frac{\sin^5 \theta_2 - \sin^5 \theta_1}{5}, \\ C_3 &= \frac{\cos^3 \theta_2 - \cos^3 \theta_1}{3}, & S_3 &= \frac{\sin^3 \theta_2 - \sin^3 \theta_1}{3}, \\ C_1 &= \cos \theta_2 - \cos \theta_1, & \Delta_0 &= \frac{\phi_2 - \phi_1}{8}, \\ \Delta_2 &= \frac{\sin 2\phi_2 - \sin 2\phi_1}{4}, & \Delta_4 &= \frac{\sin 4\phi_2 - \sin 4\phi_1}{32}, \\ \Gamma_1 &= \cos \phi_2 - \cos \phi_1, & \Sigma_1 &= \sin \phi_2 - \sin \phi_1, \\ \Gamma_2 &= \frac{\cos^2 \phi_2 - \cos^2 \phi_1}{2}, & \Sigma_2 &= \frac{\sin^2 \phi_2 - \sin^2 \phi_1}{2}, \\ \Gamma_3 &= \frac{\cos^3 \phi_2 - \cos^3 \phi_1}{3}, & \Sigma_3 &= \frac{\sin^3 \phi_2 - \sin^3 \phi_1}{3}, \\ \Gamma_4 &= \frac{\cos^4 \phi_2 - \cos^4 \phi_1}{4}, & \Sigma_4 &= \frac{\sin^4 \phi_2 - \sin^4 \phi_1}{4} \end{aligned}$$

to express the results of these integrals. The abbreviations were chosen in a way that the angular dependency can still be recognised, as C_n and Γ_n correspond to the n -th powers of the cosine of θ and ϕ , respectively, and S_n and Σ_n indicate the n -th powers of the sine of θ and ϕ .

For the results from averaging over the inclination from $-\theta$ to θ we use the abbreviations

$$C_1^0 = \cos \theta - 1 \quad , \quad C_3^0 = \frac{\cos^3 \theta - 1}{3} \quad , \quad C_5^0 = \frac{\cos^5 \theta - 1}{5} \quad .$$